SIMPLE SINGULARITIES FOR MAX-CONCAVE HAMILTON-JACOBI EQUATIONS AND GENERALIZED CHARACTERISTICS

MARTIN V. DAY AND ARIK. A. MELIKYAN

Abstract. We consider piecewise smooth viscosity solutions to a Hamilton-Jacobi equation, for which the Hamiltonian is the maximum of a finite number of smooth concave functions. We describe the possible types of "basic" singularities, namely jump discontinuities in the derivative of either the solution or the Hamiltonian which occur across a smooth hypersurface. Each such type of singularity is described in terms of properties of the Hamiltonian and the classical characteristics in the regions on either side of the singularity. Where appropriate, singular characteristic equations of the types developed by Melikyan are formulated which can be used in constructions.

1. Introduction and Overview

We consider viscosity solutions of an equation $F(x, \nabla u(x)) = 0$ with Hamiltonian F of *max-concave* type:

$$F(x, p) = -\min_i H_i(x, p). \tag{1}$$

The $H_i(x, p)$ $(i = 1, \dots, k)$ are assumed smooth (C^2) and convex in p for every fixed x. Distributing the negative, $F = \max_i(-H_i)$ and $p \mapsto -H_i(x, p)$ is concave for each i, x, explaining our choice of terminology "max-concave." Our goal is to identify the basic structures that are possible for codimension 1 singularities of piecewise smooth continuous viscosity solutions of $F(x, \nabla u(x)) = 0$ in the interior of the state space. Similar considerations are appropriate in the study of viscosity sense boundary conditions, but that topic will be taken up elsewhere.

Hamilton-Jacobi equations with F of the form (1) arise in differential games in which the minimizing player $a(t)$ can choose from only a finite number of different control settings, $a(t) \in \{1, \dots, k\}$, while the maximizing player $w(t)$ has a continuum of choices. Suppose for instance that the two players jointly determine a state trajectory in $\mathbb{R}^n$

$$\dot{x} = f(x, a(t), w(t)); \quad x(0) = x_0. \tag{2}$$

Date: February 22, 2007.

This research was supported in part by NSF grant DMS-0102266.

with resulting cost

$$J(x_0, a(\cdot), w(\cdot)) = \int_0^\tau L(x(s), a(s), w(s))\, ds + g(x(\tau)).$$

(Here τ is the time of first contact with some terminal set E, and $g : E \to \mathbb{R}$ is some given terminal cost function.) The (upper) value V of such a game will typically satisfy $F(x, \nabla V(x)) = 0$ in the viscosity sense, where F is given by (1), and the H_i are

$$H_i(x, p) = \sup_w \{\langle p, f(x, i, w)\rangle + L(x, i, w)\}. \tag{3}$$

See [5]. Such H_i are p-convex and are often smooth, depending on assumptions about f and L. See Section 4 below for an example.

Problems of this type have been considered recently in queueing theory; see [2], [3], [4], [8], [9] for instance. The minimizing controller $a(t)$ corresponds to some service priority decision, while $w(t)$ models vagaries of the load on the system. In some examples the value function has been determined through an explicit construction based on characteristic equations for the H_i. For purposes of such constructions it is important to understand the possible structures that singularities can take.

Section 2 will clarify what we mean by basic or "codimension 1" singularities, and explain some considerations related to the needs of constructing the manifolds Γ which carry the singularities. An important tool for constructing these manifolds is the *method of singular characteristics*. We provide a very brief introduction, but refer to Melikyan's monograph [11] for a more extensive treatment. Section 3 contains our description of the different basic singularity types. We use the existing terminology of "dispersal, " "equivocal," "focal," and "universal" surfaces, but also make a distinction between upward, downward, and nonsingular switching singularities because these are different from the point of view of viscosity solutions. In each case we will discuss how the manifold Γ of singularities would typically be constructed. In several cases this involves identifying a system of singular characteristics which propagate along the singular surface. It is not our purpose to offer new developments in the theory of singular characteristics, however. We will be content to identify an appropriate system of singular characteristics of one of the several standard types, but will not pursue the complications associated with possible degeneracies of that system which might occur in some examples. Finally in Section 4 we look at the extension of an example from [8] which exhibits some of the singularities discussed in Section 3.

2. Basic Singularities and Singular Characteristics

The notion of viscosity solution allows highly nonsmooth, even discontinuous, functions $u(x)$ to be considered as possible solutions. An exhaustive study of all possible types of singularities is more than can be attempted here. We impose some simplifying hypotheses about the location and structure of the singularities, limiting our scope to what are called the "simplest singularities" in [11].

2.1. **Hypotheses for Codimension 1 Singularities.** To be specific, we consider an open set $\mathcal{O} \subseteq \mathbb{R}^n$ decomposed as a disjoint union $\mathcal{O} = A \cup \Gamma \cup B$, where Γ is a smooth (C^2) manifold of dimension $n-1$ separating the remainder of $\mathcal{O}$ into disjoint open sets A and B; see Figure 1. For $x \in \Gamma$, $n(x)$ will denote the *unit normal vector* to Γ, oriented to point from A into B. Our C^2 hypothesis on Γ means that $n(x)$ is C^1. We assume that $u(x)$ is a continuous

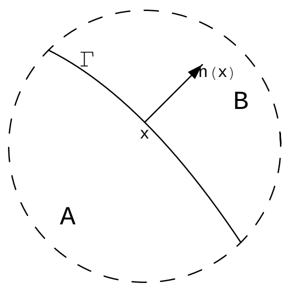

FIGURE 1. $\mathcal{O}$ and Singular Surface

function of $x \in \mathcal{O}$. We use $u_A(x)$ and $u_B(x)$ to denote the restrictions of u to A and B and respectively. These are assumed to be C^2. Their gradients $p_A(x) = \nabla u_A(x)$ and $p_B(x) = \nabla u_B(x)$ are thus C^1. We assume p_A and p_B have continuous extensions to Γ. In some cases it is reasonable to assume these extensions to Γ are smooth, and we will do so where needed for purposes of developing the singular characteristic equations. This is discussed in Section 2.3.1. We will also assume certain uniform monotonicity properties of H_i on Γ which allow us to clearly delineate between those cases where smooth extensions of $p_A(x), p_B(x)$ are reasonable and those where they are not. This hypothesis is explained in Section 2.2.2 and

We assume that $u(x)$ is a viscosity solution of

$$-\min_{i=1}^{k} H_i(x, \nabla u(x)) = 0. \tag{4}$$

The $H_i : \mathcal{O} \times \mathbb{R}^n \to \mathbb{R}$ are assumed C^2 with $p \mapsto H_i(x,p)$ convex for each x. The $i \in \{1, \dots, k\}$ will be called the *indices*. Since singular surfaces Γ often occur as the set of x where the minimizing index i in (4) changes, we want to insist that such changes are confined to Γ. Thus we assume that there is an index $i = a$ (not necessarily unique) which achieves the $\min_i$ for all $x \in A$ and a index $i = b$ which achieves the $\min_i$ for all $x \in B$. Thus for all $1 \le i \le k$ we have

$$H_a(x, p_A(x)) \le H_i(x, p_A(x)) \text{ for } x \in A;$$
$$H_b(x, p_B(x)) \le H_i(x, p_B(x)) \text{ for } x \in B.$$

It is possible that $a = b$ even though $p_A(x) \neq p_B(x)$ on Γ; see Section 3.2.1, or that $a \neq b$ even though $p_A(x) = p_B(x)$ on Γ; see Section 3.3.

2.2. **Classical Characteristics.** Since $u(x)$ is smooth on either side of Γ (A or B) it can be described by classical characteristics there. The properties of these characteristics near Γ, specifically whether they approach or leave Γ, whether they meet it transversely or tangentially, will be significant in discussing the different singularity types. In differential games such classical characteristics are typically trajectories of the state equations (2). However the minus sign in (4) is important for the correct formulation of the Hamilton-Jacobi-Isaacs equation in the viscosity sense. We need to be careful to observe the effect of the sign on the connection between the forward time directions for (2) and the classical characteristics.

The standard characteristic equations for $x(t)$ and $p(t) = \nabla u(x(t))$ associated with $F(x, \nabla u(x)) = 0$ are

$$\dot{x} = \frac{\partial}{\partial p} F(x,p), \quad \dot{p} = -\frac{\partial}{\partial x} F(x,p). \tag{5}$$

Observe that in a region (such as our A or B) where $F(x, \nabla u) = -H_i(x, \nabla u)$ for a fixed index i, the state component of (5) is

$$\dot{x} = \frac{\partial}{\partial p} F(x, \nabla u(x)) = -\frac{\partial}{\partial p} H_i(x, \nabla u(x)) = -f(x, i, w^*),$$

the last equality being in the case of (3) with w^* achieving the supremum. In the context of (2) this would be a state trajectory *in reverse time*. In most of the classical literature about singular surfaces for differential games, the various singularity types are illustrated with pictures indicating the direction of state trajectories in *forward* time; see [10], [11, Ch. 3]. We want to maintain consistency with that literature, so that the forward time direction indicated by the arrows in our figures (see the righthand pane of Figure 3 for example) corresponds to the forward time direction in state equations such as (2). For that reason, our illustrations below will indicate the direction of motion along the *reversed* characteristics. In a region where $F(x, \nabla u) = -H_i(x, \nabla u)$ these are

$$\begin{aligned} \dot{x} &= -\frac{\partial}{\partial p} F(x,p) = \frac{\partial}{\partial p} H_i(x,p), \\ \dot{p} &= +\frac{\partial}{\partial x} F(x,p) = -\frac{\partial}{\partial p} H_i(x,p). \end{aligned}$$

One can eliminate the negative in (4) by the change of dependent variable $v(x) = -u(x)$. The equivalent viscosity sense equation for $v(x)$ is $\tilde{F}(x, \nabla v(x)) = 0$ where

$$\tilde{F}(x,p) = -F(x,-p) = \min_i H_i(x,-p).$$

This $\tilde{F}$ would naturally be called *min-convex*. Thus max-concave and min-convex Hamiltonians are equivalent through this simple change of dependent variable. However, it is still the reversed characteristics for $\tilde{F}$ which correspond to the forward time direction in the state equations. Thus the min-convex reformulation offers little advantage over the max-concave view we have adopted.

Consider now the task of constructing the solution $u(x)$ by means of classical characteristics. For a game as described in the introduction, initially we would have the values $u(x) = g(x)$ prescribed at points $x = x(\tau)$ in the terminal set E, which is typically part of the boundary of the domain of $u(\cdot)$. We would then integrate backwards in time along optimal trajectories $x(t)$ to determine the values of $u(x)$ at points $x = x(t)$ which occur earlier ($t < \tau$) on those trajectories. Because of the time reversal discussed above, this corresponds to following the characteristics forward in time. In other words the *forward* characteristic direction indicates the direction of "information flow" for purposes of the construction or calculation of solutions. Since the arrows in our illustrations indicate the *reversed* characteristic direction, a typical calculation will proceed by working its way upstream, against the direction of the arrows in our illustrations. When we reach the singular surface Γ, we can no longer simply follow the classical characteristics. How we then proceed depends on the structure of the singularity. In some cases (equivocal and universal surfaces) we will need equations describing the singularity which can be used to construct Γ and the discontinuity of $\nabla u(x)$ across it before continuing with classical characteristics. The method of singular characteristics will supply us with such equations in several cases. In other cases (dispersal and nonsingular equivocal surfaces) can can expect the standard characteristics constructed prior to encountering Γ to be all we typically need to construct it.

2.2.1. *n-Monotonicity of H_i.* A simple but very important observation connects the direction of the (reversed) characteristics near Γ to properties of the relevant Hamiltonian H_i. Suppose that $x(t), p(t) = \nabla u(x(t))$ is a (reversed) characteristic on the A side of Γ, where by hypothesis $F(x, \nabla u(x)) = -H_a(x, \nabla u(x))$:

$$\dot{x} = \frac{\partial}{\partial p} H_a(x, p), \quad \dot{p} = -\frac{\partial}{\partial x} H_a(x, p),$$

and suppose that it contacts Γ at t_0: $x_0 = x(t_0) \in \Gamma$, with $p_0 = p(t_0)$. Then we have

$$\langle n(x_0), \dot{x}(t_0) \rangle = \langle n(x_0), \frac{\partial}{\partial p} H_a(x_0, p_0) \rangle = \frac{d}{d\rho} H_a(x_0, p_0 + \rho n(x_0))|_{\rho=0}. \tag{6}$$

If this quantity is positive, then because $n(x)$ points into B, we deduce that $x(t) \in A$ for $t < t_0$ and $x(t) \to x_0 \in \Gamma$ as $t \uparrow t_0$. In words, $x(t)$ *approaches* Γ on the A side. If the quantity is negative we can say $x(t)$ *departs* from Γ on the A side, meaning $x(t_0) \in \Gamma$ and $x(t) \in A$ for $t < t_0$. If the quantity is zero (and $\dot{x} \neq 0$) we can say $x(t)$ contacts Γ *tangentially.* Thus the direction of approach of a characteristic to Γ on the A side is determined by the monotonicity of $\rho \mapsto H_a(x_0, p_0 + \rho n(x_0))$ at $\rho = 0$. Similar statements apply to characteristics on the B side, except for a sign change since $n(x_0)$ points into, not out of, B.

We will say that $H_i(x_0, \cdot)$ is *n-increasing [strictly] at p_0* if the quantity in (6) is nonnegative [positive]. Similarly, $H_i(x_0, \cdot)$ is *n-decreasing [strictly] at p_0* if the quantity in (6) is nonpositive [negative]. Note that by our hypotheses, $\rho \mapsto H_i(x_0, p_0 + \rho n(x_0))$ is a smooth convex function. If (6) is 0, we consider $H_i(x_0, \cdot)$ to be both n-increasing and n-decreasing, and say $H_i(x_0, \cdot)$ is *n-tangent at p_0*. We will see in Section 3 that the viscosity solution property of $u(x)$, $x \in \Gamma$, boils down to statements about the sign of $\min_i H_i(x_0, p_A(x_0) + \rho n(x_0))$ for an appropriate range of ρ, establishing a connection between viscosity solutions and these n-monotonicity properties of the H_i.

2.2.2. *Uniform n-Monotonicity Hypothesis.* It is quite possible that (6) might change sign as x_0 varies over a singular surface. It is *not* our intent to study how such transitions between different singularity types occur, only to identify the basic types of singularities that can persist over Γ, confined to some neighborhood $\mathcal{O}$. For that reason, we assume that the signs of

$$\langle n(x), \frac{\partial}{\partial p} H_a(x, p_A(x)) \rangle \quad \text{and} \quad \langle n(x), \frac{\partial}{\partial p} H_b(x, p_B(x)) \rangle$$

are constant over $x \in \Gamma$. In other words, each of these is assumed strictly positive, identically zero, or strictly negative over Γ.

2.3. **Singular Characteristic Methodology.** For many of the singularity types considered below, we will be led to three equations which connect the values of for $u(x)$, $p = p_B(x)$ for $x \in \Gamma$:

$$F_i(x, u, p) = 0, \ i = -1, 0, 1. \tag{7}$$

Typically one of these equations will be $H_b(x, p) = 0$, and the other two describe the special features of a particular singularity type. (Dependence on u *will* occur in some instances.) We need to use these equations to construct Γ in examples. The method of singular characteristics provides a generalization of the classical method of characteristics which is suitable for this task.

To explain singular characteristics, consider again the method of classical characteristics, this time including u-dependence in the Hamiltonian. Suppose we are interested in a smooth solution to a single equation

$$F(x, u(x), \nabla u(x)) = 0, \ x \in \Omega,$$

$\Omega \subseteq \mathbb{R}^n$ being some domain. Associated with the solution is the n-dimensional manifold Σ in $\mathbb{R}^{2n+1}$ consisting of the points

$$(x, u, p) = (x, u(x), \nabla u(x)), \ x \in \Omega.$$

We need F to vanish on this manifold, *and* the differential form $du - \langle p, dx\rangle$ to vanish on its tangent space. The classical characteristic equations,

$$\dot{x} = F_p, \quad \dot{u} = \langle p, F_p\rangle, \quad \dot{p} = -F_x - pF_u, \tag{8}$$

have the property that such a manifold Σ is an invariant set, in other words if $(x(0), u(0), p(0)) \in \Sigma$ then $(x(t), u(t), p(t)) \in \Sigma$ in some interval of t values containing 0. This allows Σ to be constructed from some lower dimensional submanifold of it. See Arnold [1].

The situation for Γ and (7) is analogous. Associated with Γ and u is the $(n-1)$-dimensional manifold $\Sigma_\Gamma \subseteq \mathbb{R}^{2n+1}$ consisting of

$$(x, u, p) = (x, u(x), p_B(x)), \ x \in \Gamma. \tag{9}$$

The F_i of (7) must vanish on Σ_Γ and the differential form $du - \langle p, dx\rangle$ must vanish on its tangent space. Apart from degeneracies, this leads to a system of ODEs in $\mathbb{R}^{2n+1}$ (unique up to a scalar multiple) for which Σ_Γ is invariant, and thus can be used to construct it from a submanifold of initial points. This system takes the same form as (8), but with F replaced by the so-called *singular Hamiltonian* $\mathcal{H}$, defined by:

$$\mu\mathcal{H} = \{F_0, F_1\}F_{-1} + \{F_1, F_{-1}\}F_0 + \{F_{-1}, F_0\}F_1, \tag{10}$$

where $\mu = \mu(x, u, p)$ is a non-zero homogeneity factor and $\{\cdot, \cdot\}$ is the *Jacobi bracket* (Poisson if there is no u-dependence):

$$\{G, F\} = \langle G_x + pG_u, F_p\rangle - \langle F_x + pF_u, G_p\rangle. \tag{11}$$

This bracket occurs for instance as the derivative of $G(x, u, p)$ along the characteristic curves (8):

$$\{G, F\}(x(t), u(t), p(t)) = \frac{d}{dt}G(x(t), u(t), p(t)). \tag{12}$$

Antisymmetry, $\{F, G\} = -\{G, F\}$, is clear from (11) .

The homogeneity factor $\mu \neq 0$ in (10) can be selected arbitrarily. Although in general the choice would affect the characteristic vector field of $\mathcal{H}$ significantly, on Σ_Γ where F_i vanish it simply has the effect of rescaling the time variable, so that the resulting characteristic equations on Σ_Γ reduce to a linear combination of the respective characteristic fields for F_i:

$$\begin{aligned} \dot{x} &= \sum_{-1}^{1} \lambda_i \frac{\partial}{\partial p} F_i \\ \dot{u} &= \sum_{-1}^{1} \lambda_i \langle p, \frac{\partial}{\partial p} F_i\rangle \\ \dot{p} &= -\sum_{-1}^{1} \lambda_i \left(\frac{\partial}{\partial x} F_i + p\frac{\partial}{\partial u} F_i\right), \end{aligned} \tag{13}$$

where λ_i are $\{F_0, F_1\}/\mu, \{F_1, F_{-1}\}/\mu, \{F_{-1}, F_0\}/\mu$ for $i = -1, 0, 1$ respectively. These are the equations of singular characteristics for Σ_Γ, to be called the *MSC equations* below. Given an initial point $(x(0), u(0), p(0)) \in \Sigma_\Gamma$ it follows that $(x(t), u(t), p(t)) \in \Sigma_\Gamma$, and in particular that $u(t) = u(x(t))$ and $p(t) = p_B(x(t))$. In two dimensions ($n = 2$) we only need a single $(x(0), u(0), p(0)) \in \Sigma_\Gamma$ to reconstruct Σ_Γ locally.

These ideas are developed systematically in Melikyan [11]. The derivation of (13) depends on two nondegeneracy hypotheses (called "noncharacatericity" in [11]). First, on Σ_Γ the Jacobi brackets $\{F_i, F_j\}$ ($i \neq j$) should not simultaneously vanish. Second, on the tangent space of Σ_Γ the differential forms dF_i together with $du - \langle p, dx\rangle$ should be linearly independent. It turns out that taken together these are equivalent to the nonvanishing of the right side(s) of (13) as a vector field on Σ_Γ. See [11, Lemma 1.2]. We will assume this to hold for the MSC equations derived for the various types of basic singular surfaces Γ below, and not try to deal with what might happen at rest points of (13).

2.3.1. *Extension Hypotheses.* Observe that for the right side of the system (13) to satisfy the standard C^1 hypothesis for (local) existence and uniqueness we would want the F_i to be C^2 in a neighborhood of Γ. In some cases the F_i are constructed as Jacobi brackets of the H_i, so that we will want the H_i to be C^3 instead of just C^2. In other cases the F_i will involve $u_A(x)$ or $p_A(x) = \nabla u_A(x)$, so that we will want $u_A(x)$ to have a C^2 or C^3 extension across Γ into the region B.

Suppose that H_a is strictly n-decreasing at $(x, p_A(x))$ all $x \in \Gamma$, in other words (6) is everywhere negative on Γ. Our hypotheses insure that $u_A(x)$ extends continuously to Γ. If in fact it is C^2 on Γ, then Γ with $u_A(x)$ and $p_A(x)$ defined on it is a a noncharacteristic initial surface for the equation $H_a(x, \nabla u_A(x)) = 0$ and so by the standard theory there is a (unique) C^2 extension of $u_A(x)$ into B, solving $H_a = 0$. (Actually a neighborhood of Γ on the B side, but by reducing $\mathcal{O}$ we can assume this accounts for all of B.) When this holds we will say that $u_A(x)$ satisfies the C^2 *extension hypothesis*. If in fact this extension is such that $u_A(x)$ is C^3 throughout $\mathcal{O}$, we will say it satisfies the C^3 *extension hypothesis*. If H_b is strictly n-increasing at $(x, p_B(x))$ all $x \in \Gamma$ is strictly positive on Γ, the assumption of a C^2 extension of $u_B(x)$ to a solution of $H_b(x, \nabla u_B(x)) = 0$ throughout $\mathcal{O}$ is likewise an innocuous addition to our hypotheses, to be called the C^2 *extension hypothesis for* $u_B(x)$.

If on the other hand H_a is n-tangent at $p_A(x)$ for all $x \in \Gamma$, we can *not* generally expect $u_A(x)$ to have a C^2 extension across Γ. A hueristic argument for this is the following. The H_a characteristics which cover A can be parameterized as $x_A(s,t)$, where t is the time parameter for the characteristic equations and $s = (s_1, \ldots, s_{n-1})$ parameterize some hypersurface of initial points in A. Both $\frac{\partial x_A}{\partial(s,t)}$ and $\frac{\partial p_A}{\partial(s,t)}$ are well defined so long as $x_A(s,t) \in \mathcal{O}$. Moreover in A the Jacobian $\left|\frac{\partial x_A}{\partial(s,t)}\right| \neq 0$, but on Γ this Jacobian would vanish due to the tangency. In A, where we know $p_A(x) = \nabla u_A(x)$ is C^1, we have

$$\frac{\partial p_A}{\partial x} = \frac{\partial p_A}{\partial(s,t)} \left(\frac{\partial x_A}{\partial(s,t)} \right)^{-1}.$$

As $x_A \to \Gamma$ the p_A terms are well-behaved, but some terms of the inverse x_A-Jacobian blow up, so we can expect to encounter some singularities in $\frac{\partial p_A}{\partial x}$ on Γ. (This blow up can be observed explicitly in some examples; see for instance [9], specifically the $\bar{\alpha}_l, \bar{a}_l$ equation at the top of page 286.)

3. Catalogue of Singularity Types

We come now to our primary task of identifying the possible basic singularity types. Consider a specific $x \in \Gamma$. By continuity of u it follows that $p_A(x)$ and $p_B(x)$ have a common component τ tangential to Γ; only the normal components $\rho_i = \langle n(x), p_i(x) \rangle$ can differ.

$$p_A(x) = \tau + \rho_a n(x), \quad p_B(x) = \tau + \rho_b n(x).$$

If $\rho_a > \rho_b$, we have an *upward* singularity as illustrated in Figure 2 and discussed in subsections 3.1.*. The case of $\rho_a < \rho_b$ corresponds to a *downward* singularity as in Figure 8 and subsections 3.2.* below. If $\rho_a = \rho_b$ but the minimizing index is different on the two sides of Γ ($a \neq b$) we have a *nonsingular switching surface*, discussed in subsections 3.3.*.

A singular surface Γ such that the (reversed) characteristics depart from Γ on both sides is generally called a *dispersal surface*. These types are considered in subsections 3.*.1 below. Singular surfaces for which characteristics approach Γ from one side and depart from it on the other are called *equivocal surfaces* and discussed in subsections 3.*.2. When the characteristics approach Γ from both sides we have either a *focal surface* or a *universal surface* (in the case of $\rho_a = \rho_b$). Subsections 3.*.3 are devoted to these cases. According to our discussion at the end of Section 2.2, these characteristic approach or departure properties are connected to the n-monotonicity properties of $H_i(x, \cdot)$ for $x \in \Gamma$ and $i = a, b$. For each case our typical figure will consist of an plot (left panel) of $\rho \mapsto H_i(x, \tau + \rho n(x))$ to illustrate these monotonicity properties, and an illustration (right panel) of Γ indicating the approach/departure/tangency of the (reversed) characteristics on either side. See Figure 3 for instance.

Recall that a continuous function $u(x)$ is a *viscosity solution* to the equation

$$F(x, \nabla u(x)) = 0, \; x \in \mathcal{O} \tag{14}$$

if for every test function $\varphi \in C^1$ and every point $x \in \mathcal{O}$ at which $u - \varphi$ is a) a local minimum, or b) a local maximum, the following are satisfied (respectively):

$$\text{a) } F(x, \nabla\varphi(x)) \geq 0, \quad \text{b) } F(x, \nabla\varphi(x)) \leq 0. \tag{15}$$

Property (15a) is the *supersolution* property, and (15b) is the *subsolution* property. See [5], [6]. Under our hypotheses, this reduces to the classical notion of solution in A and B.

$$H_a(x, p_A(x)) = 0,\ x \in A; \quad H_b(x, p_B(x)) = 0,\ x \in B.$$

The issue how (15) is to be satisfied for $x \in \Gamma$.

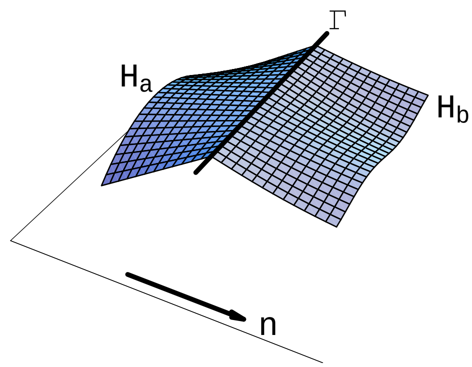

FIGURE 2. Upward Singularity for $u(x)$

3.1. **Upward Singularities.** The upward case corresponds to

$$\rho_b < \rho_a.$$

Clearly there are no smooth φ such that $u - \varphi$ has local minima at x, so the supersolution property holds vacuously. The set of $p = \nabla\varphi(x)$ such that $u - \varphi$ has a local maximum at $x \in \Gamma$ is $\overline{p_B(x), p_A(x)}$, by which we mean the line segment joining $p_B(x)$ to $p_A(x)$ in the p-plane:

$$p = \tau + \rho n(x),\ \rho_b \le \rho \le \rho_a.$$

The viscosity solution property is that $F \le 0$ for these p. For F as assumed in (1) above, this means that for every $p \in \overline{p_B(x), p_A(x)}$ we have

$$H_i(x, p) \ge 0 \text{ for all } i.$$

At the endpoints we must have equality, $H_i(x, p_i(x)) = 0$ for $i = a, b$, because $u(x)$ is a classical solution in A and B. Thus $H_b(x, \tau + \rho n(x)) = 0$ for $\rho = \rho_b$ and is nonnegative for $\rho_b < \rho < \rho_a$. This means that $H_b(x, \cdot)$ is n-increasing at $p_b(x)$. By similar reasoning $H_a(x, \cdot)$ is n-decreasing at $p_a(x)$. In particular, it is not possible for characteristics to approach Γ transversely from either side; approach is only possible tangentially. (Departure can be transverse, however.)

Unlike the downward singularities of the next section, the presence of additional indices i other than a and b does not affect the possible geometries. Once one of the geometries below is identified for a pair $i = a, b$, we simply would need to verify $H_i(x, \tau + \rho n(x)) \ge 0$ for $\rho_a \le \rho \le \rho_b$ and any additional

$i \neq a, b$ to validate the viscosity solution. Consequently our illustrations and discussion refer only to $i = a, b$. It is possible for $a = b$, but *only* if $H_a(x, \cdot)$ is n-tangent at both $p_A(x)$ and $p_B(x)$, which means $H_a(x, \cdot)$ is *not* strictly convex. The corresponds to a degenerate version in the dispersal and equivocal cases.

3.1.1. *Dispersal Surface.* The simplest possibility is for the n-monotonicites of $H_i(x, \cdot)$ at $p_i(x)$ $(i = a, b)$ to both be strict. Then we we must have the configuration illustrated in Figure 3. The strict monotonicity requires $a \neq b$. The (reversed) characteristics necessarily *depart* from Γ transversely

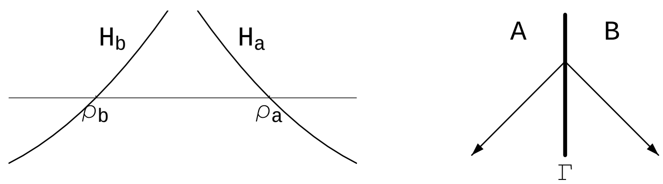

FIGURE 3. Upward Dispersal Surface

on *both* sides. Recall that in constructions we will obtain $u_A(x)$ and $u_B(x)$ by integrating backwards along the (reversed) characteristics. Thus we will have both $u_A(x)$ and $u_B(x)$, and the H_a and H_b characteristic curves associated with them respectively, in hand as we seek to identify Γ. If we make the C^2 extension hypotheses for both u_A and u_B (see Section 2.3.1), these characteristic families will extend $u_A(x)$ and $u_B(x)$ to a neighborhood of Γ. The singular surface will then be obtained simply as the intersection of the graphs,

$$\Gamma = \{x : \ u_A(x) = u_B(x)\}.$$

Smoothness of Γ follows from the implicit function theorem. Curves $x(t)$ tracing Γ are characterized by $\dot{x} \perp (p_A(x) - p_B(x))$. Thus there is no practical need for MSC equations to describe Γ in this case.

Degenerate versions of this case (departure from Γ from both sides) are possible if one or both of $H_i(x, p)$ are n-tangent at $p_i(x)$. The case of tangency for $i = b$ but strict monotonicity for $i = a$ is illustrated in Figure 4. Such a degenerate dispersal surface would still be discovered as

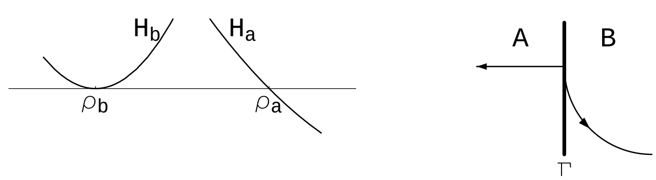

FIGURE 4. Degenerate Dispersal Surface

one integrates the characteristic equations in both A and B backwards from initial conditions given elsewhere. Γ would occur *both* as the locus of $u_A(x) = u_B(x)$ *and* as an envelope of the characteristics on the B side. The occurrence of such structure would simply be a remarkable coincidence, but nothing more. Tangency for both $i = a, b$ with departure from Γ on both sides would be a doubly remarkable coincidence.

3.1.2. *Equivocal Surface.* If we have n-tangency of $H_i(x, \cdot)$ on at least one side of Γ, other types of upward singular surfaces are possible. Suppose H_b is n-tangent at $p_B(x)$, while H_a remains strictly n-decreasing at $p_A(x)$. This makes it possible for the B-side characteristics to *approach* Γ, provided they do so tangentially. This is illustrated in Figure 5. (The significant difference from Figure 4 is the direction of the (reversed) characteristics in B.) In this case Γ is an equivocal surface. (Other configurations producing equivocal surfaces are found in Sections 3.2.2 and 3.3.2 below)

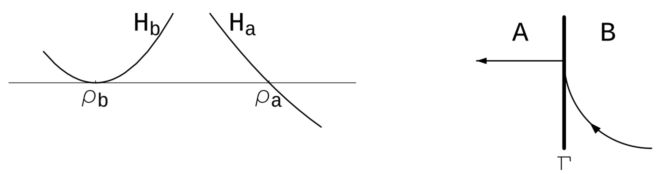

FIGURE 5. Upward Equivocal Surface

One would construct such a solution by first integrating the H_a characteristic equations from initial conditions given elsewhere to generate $u_A(x)$ and $p_A(x) = \nabla u_A(x)$ in A up to and on Γ. Then one must apply the discontinuity in $\nabla u(x)$ across Γ to obtain $p_B(x)$ on Γ and resume, integrating the H_b characteristic equations into B. This is tricky in practice because the characteristic equations in A offer no clue that the singular surface is present; it is a globally determined feature. However, given that $x \in \Gamma$ is such a point, Γ can be "tracked" using the appropriate MSC equations. Suppose we already know $u_A(x)$ and $p_A(x)$ in $A \cup \Gamma$. Since the H_a characteristics for $u_A(x)$ in A meet Γ nontangentially, it is reasonable to invoke the extension hypothesis of Section 2.3.1 to extend the $u_A(x)$ and $p_A(x)$ across Γ into B, still solving $H_a = 0$.

Our task is to identify Γ and the values of $p_B(x)$. In other words we need to find the manifold Σ_Γ of (9). We can identify three equations describing Σ_Γ under the circumstances we have assumed. First, for $(x, u, p) \in \Sigma_\Gamma$ we have

$$u - u_A(x) = 0.$$

Secondly, because $p = p_B(x)$ we must have

$$H_b(x, p) = 0.$$

Thirdly, we know that $p_B(x) - p_A(x)$ is normal to Γ at x. The n-tangency of H_b in Figure 5 means that the normal component of $\frac{\partial}{\partial p} H_b(x, p_B(x))$ is

$= 0$. It is therefore necessary that $p = p_B(x)$ satisfy

$$\langle \frac{\partial}{\partial p} H_b(x,p), p - p_A(x) \rangle = 0.$$

Viewing $u_A(x)$ and $p_A(x)$ as known functions, these give us three equations (7) describing the manifold Σ_Γ associated with our upward equivocal surface Γ:

$$\begin{aligned} F_1(x,u,p) &= u - u_A(x), \\ F_0(x,u,p) &= H_b(x,p), \\ F_{-1}(x,u,p) &= \langle \frac{\partial}{\partial p} H_b(x,p), p - p_A(x) \rangle. \end{aligned} \tag{16}$$

(Notice that for F_{-1} to be C^2 we need H_b and the extended $u_A(x)$ to be C^3. Then F_1 is C^2 as well.)

Equations (16) lead to a standard type of singular characteristic system; see [11, (1.88)]. A simple calculation shows that

$$\{F_1, F_0\} = F_{-1},$$

which vanishes on Σ_Γ, so the λ_{-1} term in (13) vanishes. Also, since H_b has no u-dependence, the $\frac{\partial}{\partial u} F_0$ term vanishes. Provided $\{F_1, F_{-1}\} \neq 0$ we can take it as the homogeneity factor μ. The MSC equations simplify to

$$\begin{aligned} \dot{x} = \frac{\partial}{\partial p} H_b, \quad \dot{u} &= \langle p, \frac{\partial}{\partial p} H_b, \rangle, \\ \dot{p} = -\frac{\partial}{\partial x} H_b &- \frac{\{F_0, F_{-1}\}}{\{F_{-1}, F_1\}}(p - p_A). \end{aligned} \tag{17}$$

It is only the last term of $\dot{p}$ which makes (17) different from the H_b characteristic system in B. (The expressions for $\{F_0, F_{-1}\}$ and $\{F_{-1}, F_1\}$ involve the Hessian of $u_A(x)$ and second order partials of H_b. They are not particularly illuminating, so we have not written them out.)

Having identified Γ and $p_B(x)$ defined on it, we would then use the standard H_b characteristic equations taking $x \in \Gamma$, $u = u_A(x)$, $p = p_B(x)$ as initial conditions, and solve (forward) to obtain $u_B(x)$ and $p_B(x)$ for $x \in B$. If the configuration we have described (Figure 5) is truly present, this will complete the construction of $u(x)$ and Γ in $\mathcal{O}$. We will see an example of this kind of equivocal surface in the example of Section 4 below.

A degenerate form of this case is possible, in which we also have tangency for $i = a$. This is illustrated in Figure 6. In this case Γ would be easy to locate as the envelope of the characteristics from the A side, so MSC equations are not needed. With Γ and its normals $n(x)$ in hand, we would find $p_B(x)$ as $p_B(x) = p_A(x) + \rho n(x)$ for a scalar $\rho < 0$ determined by solving $H_b(x, p_B(x)) = 0$.

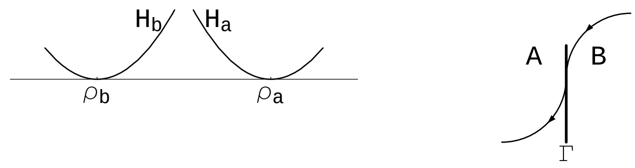

FIGURE 6. Degenerate Equivocal Surface

3.1.3. *Focal Surface.* The remaining basic upward singularity type occurs when both $H_i(x, \cdot)$ are tangent to 0 at $p_i(x)$ and the reversed characteristics *approach* Γ tangentially on *both* sides; see Figure 7. This is typically called a focal surface, and is the most difficult type of singular surface to construct. One must simultaneously identify the $x \in \Gamma$ and the pair $p_A(x), p_B(x)$. There are multiple equations that must hold on Γ:

$$\begin{aligned} H_a(x, p_A(x)) = 0, \quad H_b(x, p_B(x)) = 0, \\ \langle \frac{\partial}{\partial p} H_a(x, p_A(x)), p_B(x) - p_A(x) \rangle = 0, \\ \langle \frac{\partial}{\partial p} H_b(x, p_B(x)), p_B(x) - p_A(x) \rangle = 0, \end{aligned}$$

along with the fact that $p_B(x) - p_A(x)$ is normal to Γ. This is outside the scope of the standard method of singular characteristics, as we have summarized it above. One approach involves a coupled pair of PDEs describing $p_A(x)$ and $p_B(x)$ on Γ; see [12]. We cannot offer any further discussion of constructive approaches here.

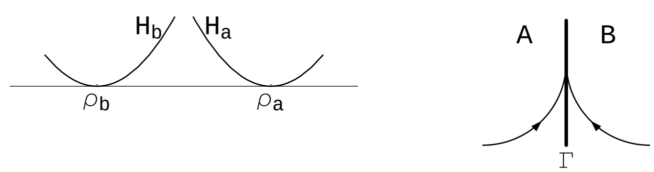

FIGURE 7. Upward Focal Surface

3.2. **Downward Singularities.** We now turn our attention to singularities of the "downward" type, as illustrated in Figure 8. The normal component ρ of p must have an upward jump as we move across the singular curve Γ in the normal direction:

$$\rho_a < \rho_b.$$

Now there exist no smooth φ so that $u - \varphi$ has a local max at x. The subsolution property is thus vacuous. The set of $p = \nabla\varphi(x)$ such that $u - \varphi$ has a local min at x is the line segment $\overline{p_A(x), p_B(x)}$. The supersolution

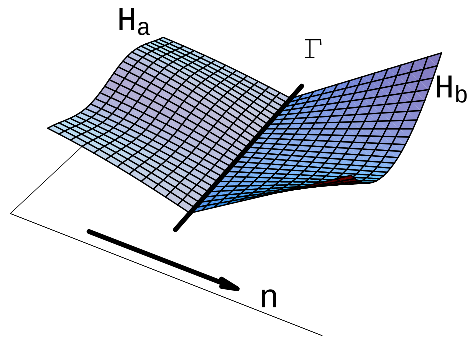

FIGURE 8. Downward Singularity

property requires $F \geq 0$ for these p. For F as assumed above, this means that for each p in $\overline{p_A(x), p_B(x)}$ we must have

$$\min_i H_i(x,p) \leq 0.$$

In other words, for each $\rho_a \leq \rho \leq \rho_b$ these is some index i for which $H_i(x, \tau + \rho n(x)) \leq 0$. We also have $H_i = 0$ at the endpoints: $i = a$ for ρ_a and $i = b$ for ρ_b. Indices i other than those which give the minimum are completely irrelevant for such a viscosity solution. A single $i = a = b$ could be responsible for the minimum for all $p \in \overline{p_A(x), p_B(x)}$ as in Figure 10. In other situations two or more i may be involved, as illustrated in Figure 9. The case of a focal surface, Section 3.2.3, while possible for a single i, will typically require at least three distinct indices $i = a, b, c$; see Figure 11.

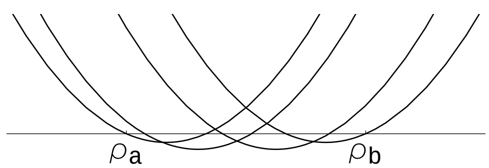

FIGURE 9. Multiple Minimizing Indices

3.2.1. *Dispersal Surface.* This is the case in which $H_a(x, \cdot)$ is $n(x)$-decreasing at $p_A(x)$ and $H_b(x, \cdot)$ is $n(x)$-increasing at $p_B(x)$. Figure 10 illustrates, assuming strict monotonicites and using a common index $a = b$. However it is possible for $a \neq b$, with yet other i involved to achieve $\min_i H_i \leq 0$ as in Figure 9. Strict monotonicity for the endpoints implies that the (reversed) characteristics *depart* from Γ (transversely) on both sides. As in the other

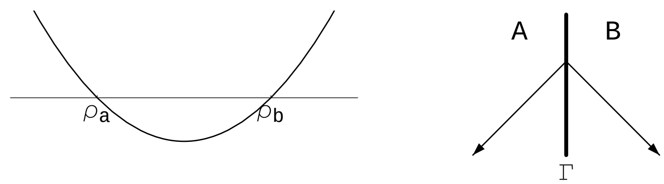

FIGURE 10. Downward Dispersal Surface

dispersal surfaces above, Γ would easily be identified in a construction as the set where $u_A(x) = u_B(x)$, the u_i obtained by integrating the characteristic equations from initial data elsewhere. Degenerate versions are possible, with n-tangency at either or both ends. As in Section 3.1.1, these would be merely remarkable coincidences of the locus of $\Gamma = \{x : \; u_A(x) = u_B(x)\}$ with the envelope(s) of the characteristics on one (or two) sides.

3.2.2. *Equivocal Surface.* This is the case in which $H_i(x, \cdot)$ is $n(x)$-decreasing at $p = p_i(x)$ for both $i = a$ and $i = b$, leading to another type of equivocal surface. The typical case in which both n-monotonicities are strict is illustrated in Figure 11.

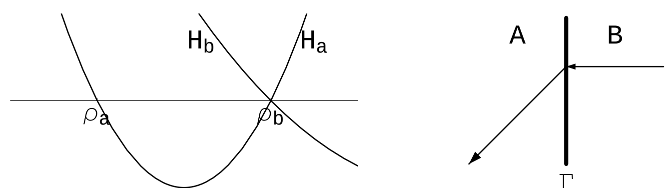

FIGURE 11. Downward Equivocal Surface

Just as for the previous type of equivocal surface, the presence of Γ may be difficult to recognize in calculations. Once its presence is suspected however, MSC equations allow Γ to be tracked from initial points $x_0 \in \Gamma$. Assume $u_A(x)$ and $p_A(x)$ are already in hand for the A side of Γ. For the non-degenerate case, assume the n-monotonicity of H_a at $p_A(x)$ is strict. The geometry of the singularity implies the following equations for $u = u_A(x)$ and $p = p_B(x)$ on the B side of Γ:

$$H_{a'}(x, p) = 0, \quad H_b(x, p) = 0, \quad \text{and } u - u_A(x) = 0.$$

Here $a' = a$ if as in Figure 11 there are no indices other that a, b involved. If however the situation is as in Figure 12, a' is the index for the minimizing H_i for the interval $(\rho_b - \epsilon, \rho_b)$ just to the left of ρ_b in the figure. We now form the MSC equations (13) using

$$F_0 = H_b, \quad F_{-1} = H_{a'}, \quad F_1(x, u, p) = u - u_A(x).$$

For F_1 to be C^2 we need to invoke the C^2 extension hypothesis for $u_A(x)$, as described in Section 2.3.1. This is another common type of singular surface;

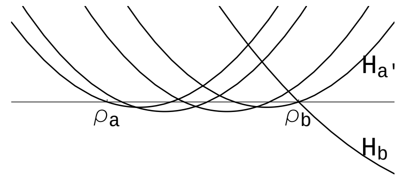

FIGURE 12. Downward Equivocal Surface with Multiple Indices

see [11, (1.95)]. Taking the homogeneity factor to be

$$\mu = \{F_0, F_1\} + \{F_1, F_{-1}\} = \{H_b, F_1\} - \{H_{a'}, F_1\},$$

the resulting system of singular characteristics can be written

$$\begin{aligned} \dot{x} &= \lambda_1 \frac{\partial}{\partial p} H_{a'} + \lambda_2 \frac{\partial}{\partial p} H_b, \quad \dot{u} = \lambda_1 \langle p, \frac{\partial}{\partial p} H_{a'} \rangle + \lambda_2 \langle p, \frac{\partial}{\partial p} H_b \rangle, \\ \dot{p} &= -\lambda_1 \frac{\partial}{\partial x} H_{a'} - \lambda_2 \frac{\partial}{\partial x} H_b - (\{H_{a'}, H_b\}/\mu)(p - p_A(x)), \end{aligned} \tag{18}$$

where

$$\lambda_1 = \{H_b, F_1\}/\mu, \quad \lambda_2 = -\{H_{a'}, F_1\}/\mu.$$

Degenerate versions are possible. Tangency on the B side corresponds to

$$0 = \langle p - p_A(x), \frac{\partial}{\partial p} H_b \rangle = \{F_1, F_0\},$$

which implies $\lambda_1 = 0$ as well. If present, this should just emerge as the MSC equations generate Γ. If H_a is n-tangent at $p_A(x)$ (all along Γ) then Γ is an envelope for the A-characteristics and we would identify it by that property.

3.2.3. *Focal Surface.* A focal surface occurs if the characteristics *approach* Γ from both sides. This requires that $H_a(x, \cdot)$ is n-increasing at $p_A(x)$ and that $H_b(x, \cdot)$ is n-decreasing at $p_B(x)$. If these are strict monotonicities, then $a \neq b$ and at least one additional index i is needed to account for $\min_i H_i \leq 0$ for $\rho_a \leq \rho \leq \rho_b$, as illustrated in Figure 13. Once again, degenerate versions are possible if n-tangencies occur for H_a or H_b. As for the upward focal surface of Section 3.1.3, the construction of such a surface requires a system of simultaneous equations for Γ and both $p_A(x), p_B(x)$ for $x \in \Gamma$, which is beyond the scope of the standard type of MSC equations. We refer again to [12].

3.3. **Nonsingular Switching Surfaces.** We assumed above that $p_A(x) \neq p_B(x)$ for $x \in \Gamma$. We now consider the possibilities in which $p_A(x) = p_B(x)$, $x \in \Gamma$. This makes $u(x)$ a C^1 function throughout $\mathcal{O} = A \cup \Gamma \cup B$ and a classical solution of our equation $F(x, \nabla u(x)) = 0$. But there still can be a significant singularity if the minimizing index changes across Γ: $a \neq b$. In this case we will refer to Γ as a *nonsingular switching surface.* These can be viewed as limiting versions of certain cases above in which $\rho_b - \rho_a \to 0$.

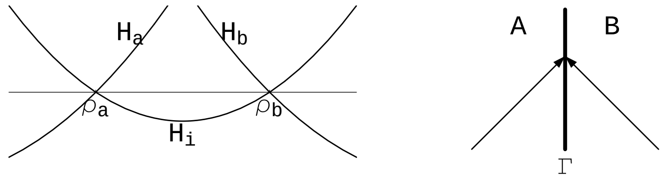

FIGURE 13. Downward Focal Surface

3.3.1. *Dispersal Surface.* This is the limiting version of the dispersal surface of Section 3.1.1. $H_a(x, \cdot)$ is n-decreasing at $p_A = p_B(x)$ while $H_b(x, \cdot)$ is n-increasing. Figure 14 illustrates the structure in the case of strict monotonicites. As always, degenerate versions are possible in which one or the other of H_i is n-tangent. As for all other dispersal surfaces, Γ would be identified as $\Gamma = \{x : u_A(x) = u_B(x)\}$ with both u_A and u_B determined from classical characteristics with initial conditions elsewhere. No MSC equations are necessary. (In fact it is also necessary that $H_b(x, p(x)) = H_a(x, p(x))$ holds on Γ, making this type of singularity overdetermined, and thus unlikely to occur.)

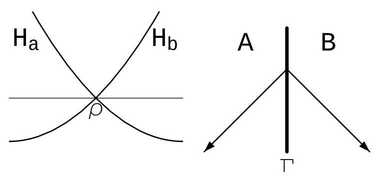

FIGURE 14. Nonsingular Dispersal Surface

3.3.2. *Equivocal Surfaces.* If both H_i are $n(x)$-decreasing at $p_A = p_B$, we have an equivocal surface, as in Figure 15. A degenerate version, in which H_b is n-tangent, Figure 16, can be viewed as a limiting version of Section 3.1.2. With $u_A(x)$ and $p_A(x)$ in hand (from the A-side characteristics initiated elsewhere), we can locate Γ simply as the locus of

$$H_b(x, p_A(x)) = 0,$$

so no MSC equations are needed. Section 4.2 below provides an example.

3.3.3. *Universal Surface.* This final type of nonsingular switching surface is the limiting version of the focal surface of Section 3.2.3, with characteristics approaching Γ from both sides. With the additional property that $p_A(x) = p_B(x)$, as we have here, this is called a universal surface. We have $H_a(x, \cdot)$ n-increasing at $p_A(x) = p_B(x)$, while $H_b(x, \cdot)$ is n-decreasing at the same value. Figure 17 illustrates for strict monotonicities. (The additional $i \neq a, b$ of Figure 3.2.3 is now irrelevant.)

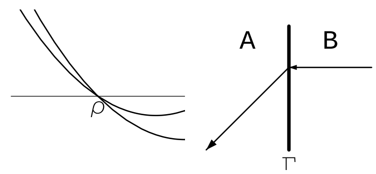

Figure 15. Nonsingular Equivocal Surface

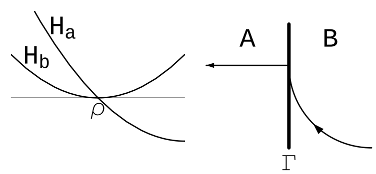

Figure 16. Degenerate Nonsingular Equivocal Surface

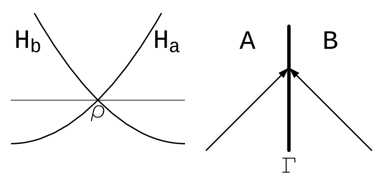

Figure 17. Universal Surface

In this situation (like the focal surfaces above) we have neither $u_A(x)$ or $u_B(x)$ to work with in developing MSC equations that can be used in constructing Γ. However, since $p_A(x) = p_B(x)$ on Γ there is only one p value associated with each $x \in \Gamma$. This puts us back in the situation of determining a manifold Σ_Γ as in (9), for which MSC equations *are* a suitable tool. Two equations are clearly necessary for $x \in \Gamma$ and the corresponding $p = p_A(x) = p_B(x)$:

$$F_1 = H_a(x, p) = 0, \quad F_0 = H_b(x, p) = 0 \tag{19}$$

A third equation follows from the assumed approach to Γ by the (reversed) characteristics on both sides and the change in minimizer from H_a to H_b as we cross Γ. On the A side the (reversed) H_a characteristics move from the interior of A to points of contact with Γ. We have $H_b - H_a \geq 0$ in A and $H_b - H_a = 0$ on Γ. Therefore the derivative of $H_b - H_a$ along the (reversed) H_a characteristic must be nonpositive at the point where the characteristic meets Γ:

$$0 \geq \frac{d}{dt}(H_b - H_a)(x(t), p(t)) = -\{H_b - H_a, H_a\} = -\{H_b, H_a\}.$$

(We have used (12) to evaluate the total derivative along the characteristic, with the negation for the time reversal, and the the fact that $\{H_a, H_a\} = 0$ due to antisymmetry.) Thus $\{H_b, H_a\} \geq 0$ at points of Σ_Γ. Reversing the roles of H_a and H_b, the same argument applies on the B side, implying that $-\{H_b, H_a\} = \{H_a, H_b\} \geq 0$. We conclude that $\{H_b, H_a\} = 0$ on Σ_Γ. This is our third equation for Σ_Γ:

$$F_{-1} = \{H_b, H_a\} = 0. \tag{20}$$

The MSC system for these F_i is again a familiar one; see [11, (1.90)]. Note that in reference to (13) we have $\{F_0, F_1\} = F_{-1} = 0$ on Γ, so that the λ_{-1} terms drop out of (13) on Γ. A convenient choice of homogeneity factor is $\mu = \{F_1, F_{-1}\} + \{F_{-1}, F_0\}$. The MSC system (13) is then

$$\begin{aligned} \dot{x} = \lambda_0 \frac{\partial}{\partial p} H_b + \lambda_1 \frac{\partial}{\partial p} H_a, \quad \dot{u} = \lambda_0 \langle p, \frac{\partial}{\partial p} H_b \rangle + \lambda_1 \langle p, \frac{\partial}{\partial p} H_a \rangle, \\ \dot{p} = -\lambda_0 \frac{\partial}{\partial x} H_b - \lambda_1 \frac{\partial}{\partial x} H_a, \end{aligned} \tag{21}$$

Such universal surfaces have occurred frequently in recent examples from queueing theory. We will see one in Section 4.1 below. (One also occurs as "F" in [8, Figure 4], although no details are provided there.)

4. An Example

We mentioned in the introduction that recent asymptotic studies of queuing networks have led to consideration of differential games whose HJI equations are of the max-concave form here. In this section we look one such example in which some singular surfaces of the types mentioned above occur. This is an extension of the example described in Section 6 of [8]. In that work the problem was considered only in the small triangular region of the first quadrant below the dashed line in Figure 18 below. One reason for the domain restriction was that the discussion of [8] was limited to smooth solutions. Here we consider the extension of that solution to the larger region of the first quadrant covered by the characteristics illustrated in Figure 18. In this larger region singularities do occur. We are not interested in identifying this particular solution as the unique solution to some precisely formulated differential game, or in discussing the associated boundary conditions on the coordinate axes. Rather we are only interested in observing that this example exhibits some of the singularity types described above.

The example is planar: $n = 2$. There just two indices: $i = 1, 2$. The H_i are determined as in (3) using

$$f(x, i, w) = w - g_i, \quad L(x, i, w) = \frac{1}{2}|x|^2 - \frac{1}{2}|w|^2,$$

where the g_i are the vectors

$$g_1 = (2, 1), \quad g_2 = (1/2, 2).$$

This gives

$$H_i(x,p) = \frac{1}{2}|p|^2 - \langle p, g_i\rangle + \frac{1}{2}|x|^2$$

Using these we form the max-concave Hamiltonian (1).

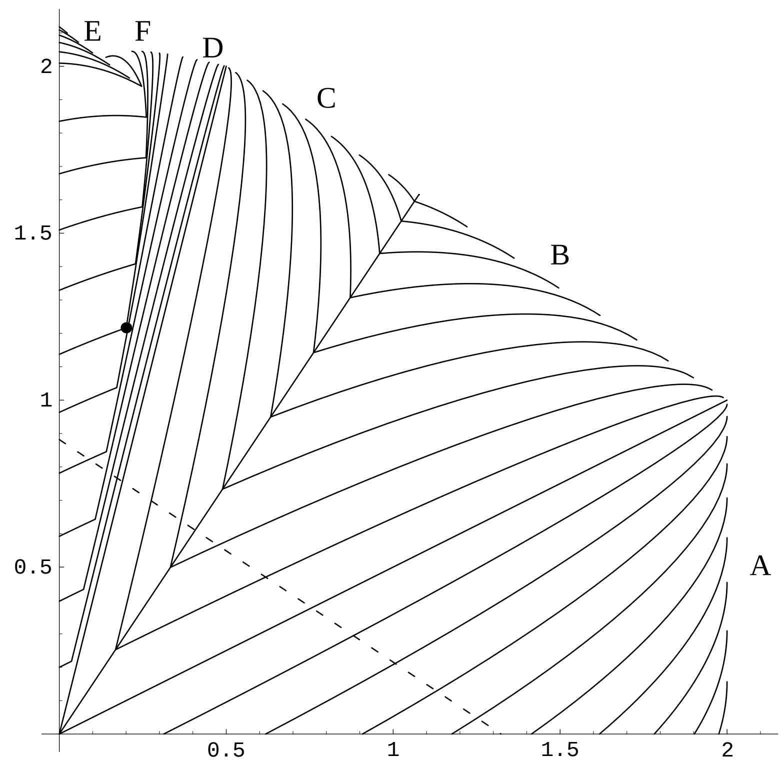

Figure 18. Queueing Example

Figure 18 shows the family of characteristics from which the solution of interest is constructed. We discuss below the several singular characteristics evident here.

4.1. **A Universal Surface.** The line separating regions B and C is a universal surface Γ as described in Section 3.3.3. It is easily located by solving the three equations (19) and (20) algebraically.

$$H_1 = 0, \quad H_2 = 0, \quad \{H_1, H_2\} = 0.$$

Working out the bracket, we find

$$0 = \{H_1, H_2\} = \langle x, g_1 - g_2\rangle.$$

We also find that

$$0 = H_2 - H_1 = \langle p, g_1 - g_2\rangle.$$

Thus on the manifold Σ_Γ associated with Γ both x and p are constrained to the 1-dimensional subspace of $\mathbb{R}^2$ orthogonal to $g_1 - g_2$. A convenient basis vector for this subspace is the following convex combination of g_i:

$$\eta = \lambda_0 g_1 + \lambda_1 g_2 = \frac{7}{13}(2,3), \quad \lambda_0 = 5/13,\ \lambda_1 = 8/13. \tag{22}$$

This has the property that

$$\langle \eta, g_1\rangle = \langle \eta, \eta\rangle = \langle \eta, g_2\rangle.$$

Along Γ we have $x = c\eta$ and $p(x) = b\eta$ for scalars c, b. Plugging into $H_i(x, p(x)) = 0$ implies $b = 1 - \sqrt{1-c^2}$. (The alternate choice of $b = 1 + \sqrt{1-c^2}$ does not correspond to the solution pictured in the figure.) This completely determines Σ_Γ as a (nonlinear) manifold in $\mathbb{R}^5$ whose x-projection Γ into $\mathbb{R}^2$ is the ray from the origin generated by η. The graphs of H_i in the normal direction to Γ at such $(x, p(x))$ are precisely as illustrated in Figure 17, with $a = 2$ on the left or C side and $b = 1$ on the right.

Although we did not need the MSC equations (21) to construct Σ_Γ, it is a simple matter to check them. With $a = 2$, $b = 1$ the x and p-equations work out as

$$\begin{aligned} \dot{x} &= \lambda_0(p - g_1) + \lambda_1(p - g_2) \\ \dot{p} &= -\lambda_0 x - \lambda_1 x, \end{aligned}$$

where $\lambda_0 = \{F_1, F_{-1}\}/\mu$ and determined from $\lambda_1 = \{F_{-1}, F_0\}/\mu$ are

$$\{F_1, F_{-1}\} = \langle g_1 - g_2, p - g_2\rangle,\ \{F_{-1}, F_0\} = \langle g_1 - g_2, g_1 - p\rangle,\ \mu = |g_1 - g_2|^2.$$

With $p = b\eta$ we find that $\lambda_0 = \{F_1, F_{-1}\}/\mu$ and $\lambda_1 = \{F_{-1}, F_0\}/\mu$ work out to be exactly the constant values used in (22) above. The differential equations for $x = c\eta$ and $p = b\eta$ reduce to equations for the scalar coefficients:

$$\dot{c} = b - 1, \quad \dot{b} = -c.$$

The solution corresponding to our Σ_Γ is

$$c(t) = -\sin(t), \quad b(t) = 1 - \cos(t), \quad t \in (-\pi/2, 0).$$

4.2. **A Nonsingular Equivocal Surface.** The construction of the solution in regions E, F, and D depends on $p(x)$ for $x = (0, x_2)$ on the vertical axis. The determination of these values involves the use of special singular characteristic equations associated with oblique derivative boundary conditions. The interested reader may consult [8], [7] for more on this. For our purposes here we simply exhibit the appropriate values of $p(x)$ on the vertical axis:

$$p(0, x_2) = \frac{1}{2}\left(3 - \sqrt{9 - 2x_2^2}\right)(1,1) \quad \text{(vector with equal components)}.$$

This satisfies $H_1(x, p(x)) = 0$ for $x = (0, x_2)$. With these as initial conditions, the region E is then covered by H_1 characteristics producing $u_E(x)$ and $p_E(x) = \nabla u(x)$ in that region. However $i = 1$ is minimizing $(0 = H_1 \leq H_2)$ only in a neighborhood of the vertical axis, not in the full region covered by these characteristics. As in Section 3.3.2, the locus of $0 = H_2(x, p_E(x))$ is a nonsingular equivocal curve Γ with the structure illustrated in Figure 15. A portion of this curve is visible in Figure 18 as the boundary between regions E and D, below the point $x^* \approx (.20, 1.22)$ marked with a solid dot. The characteristics which cross this singular curve below x^* are continuous in p, $p_D(x) = p_E(x)$, and continue into region D with H_2 minimizing. However, if we observe the H-plots (as on the left in Figure 15) moving $x \in \Gamma$ upward toward x^* we observe that the H_b ($b = 2$) graph flattens out, approaching the situation of Figure 16. The plots are provided in the top row of Figure 19, with the lower left plot being for x^* itself.

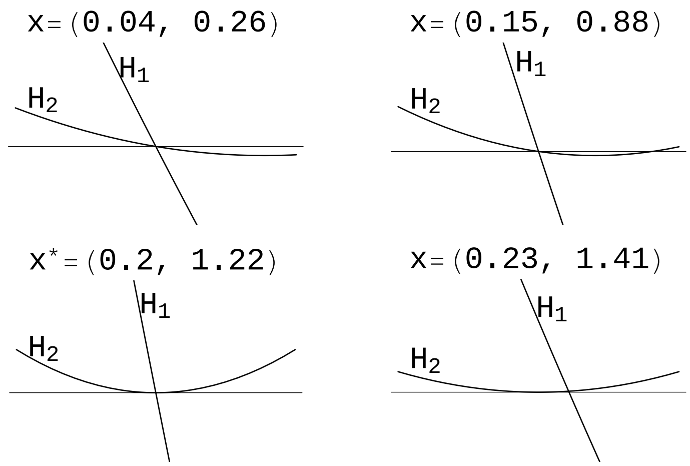

FIGURE 19. “Bifurcation” of Equivocal Surface

4.3. **An Upward Equivocal Surface.** At the point x^* we have a sort of bifurcation in the H-plot. The situation here is a limiting version an an upward equivocal surface as in Section 3.1.2, Figure 5, in which $\rho_b = \rho_a$. With $p_E(x)$ in the role of p_A, we now extend Γ beyond (above) x^* so as to satisfy equation (16) (with $p = p_E(x^*)$ at x^* itself). The result of this extension appears above x^* in Figure 18 as the boundary between regions E and F, with a typical H-plot in the lower right of Figure 19. The characteristics in region F are those using H_2 with initial conditions on Γ and the p values for the H_2 side of Γ as produced by our solution of (16).

The location of Γ itself is determined by solving the MSC equations (17) with the initial point $x_0 = x^*$ and $p_0 = p_E(x^*)$. However, for this particular example we can use (16) to develop a simpler two dimensional system describing Γ, instead of the four dimensional system resulting from (17). Given $u_E(x)$ and $p_E(x)$ for $x \in \Gamma$, we seek the value $p = p_F(x)$. We know that $p - p_E(x)$ is is normal Γ. Our equation for Γ will simply be an expression of $\dot{x} \perp (p - p_E(x))$. The second equation of (16) can be expressed as

$$\begin{aligned} 0 = H_2(x,p) &= \frac{1}{2}\left[|p-g_2|^2 - (|g_2|^2 - |x|^2)\right] \\ &= \frac{1}{2}\left[|p-g_2|^2 - r(x)^2\right], \quad \text{where } r(x) = (|g_2|^2 - |x|^2)^{1/2}. \end{aligned}$$

In other words,

$$|p - g_2| = r(x).$$

The third equation of (16) says

$$0 = \langle \frac{\partial}{\partial p} H_2(x,p), p - p_E(x)\rangle = \langle p - g_2, p - p_E(x)\rangle.$$

In the plane, these two equations determine p up to one of two possibilities. A trigonometric calculation leads to the expression

$$p - g_2 = \frac{r(x)}{|p_E(x)(x) - g_2|^2} \cdot \begin{bmatrix} r(x) & +\sqrt{2H_2(x,p_E(x))} \\ -\sqrt{2H_2(x,p_E(x))} & r(x) \end{bmatrix} (p_E(x) - g_2). \tag{23}$$

(For the alternate solution the signs of the off-diagonal terms are reversed. The Γ resulting from that turns out to be untenable, because it lies farther to the right, requiring $u = u_E$ to be used beyond the region in which $H_1(x, p_E(x)) \le H_2(x, p_E(x))$ holds.) Since $p - g_2$ is orthogonal to $p - p_E(x)$, the right side of (23) is tangent to Γ. So we can simply take the right side of (23) as the definition of a vector field $\Phi(x)$. Γ is then obtained by solving $\dot{x} = \Phi(x)$ with the bifurcation point x^* as the initial condition.

Actually, the construction described at the beginning of Section 4.2 doesn't produce $p_E(x)$ as an explicit function of x, but rather as an expression in terms of a pair of parameters: s parameterizing the vertical axis, and t parameterizing the solution of the H_1 characteristic in region E starting from the point on the boundary with parameter value s. Let $x_E(s,t)$ refer to the parameterization of the state variable x associated with this family of H_1 characteristics. We must solve our ODE for Γ using its description in this parameterization:

$$\frac{\partial x_E(s,t)}{\partial(s,t)} \begin{bmatrix} \dot{s} \\ \dot{t} \end{bmatrix} = \Phi(x_E(s,t)).$$

Computing and then inverting an explicit expression for $\frac{\partial x_E(s,t)}{\partial(s,t)}$ produces the actual ODE which when solved (numerically) produces a parametric description of Γ in the form $x_E(s(\tau), t(\tau))$.

In summary, the construction of this solution in regions E, F, and D begins with computing u along the vertical axis to obtain the values of u and $p = \nabla u$ satisfying certain boundary conditions [8] on that axis, then extending into the interior using conventional characteristics until the equivocal curve(s) on the right boundary of region E is reached. The lower portion of that curve is a nonsingular equivocal or "switching" curve; p is extended across it by continuity. The upper portion of that curve is a singular equivocal curve which is located by the MSC equations (reformulated in parameter space) and which prescribes the p discontinuity across the curve. Once past the switching/singular curve, conventional characteristics provide the extension through regions D and F. This illustrates how our study of singularity structures for viscosity solutions and their MSC descriptions can be important for explicit solutions in particular examples.

References

[1] Arnold, V.I., Geometrical Methods in the Theory of Ordinary Differential Equations, Springer Verlag, New York, 1988.

[2] R. Atar and P. Dupuis, *A differential game with constrained dynamics and viscosity solutions of a related HJB equation*, Nonlinear Analysis **51** (2002), pp. 1105–1130.

[3] R. Atar, P. Dupuis and A. Schwartz, *An escape time criterion for queueing networks: Asymptotic risk-sensitive control via differential games*, Math. of Op. Res. **28** (2003), pp. 801–835.

[4] J. A. Ball, M. V. Day, and P. Kachroo, *Robust feedback control of a single server queueing system*, Mathematics of Control, Signals, and Systems **12** (1999), pp. 307–345.

[5] M. Bardi and I. Cappuzzo-Dolcetta, Optimal Control and Viscosity Solutions of Hamilton-Jacobi-Bellman Equations, Birkhäuser, Boston, 1997.

[6] Crandall, M.G., Ishii, H., Lions, P.L.: *User's guide to viscosity solutions of second order partial differential equations*, Bull. A.M.S. **27**(1992), pp. 1–67.

[7] M. V. Day, *On Neumann type boundary conditions for Hamilton-Jacobi equations in smooth domains*, Applied Mathematics and Optimization, **53** (2006), pp. 359–381.

[8] M. V. Day, *Boundary-influenced robust controls: two network examples*, ESAIM: Control, Optimisation and Calculus of Variations, **12** (2006), pp. 662–698.

[9] M. V. Day, J. Hall, J. Menendez, D. Potter and I. Rothstein, *Robust optimal service analysis of single-server re-entrant queues*, Computational Optimization and Applications, **22** (2002), pp. 261–302.

[10] R. Isaacs, Differential Games, Wiley, New York, 1965.

[11] A. Melikyan, Generalized Characteristics of First Order PDEs: Applications in Optimal Control and Differential Games. Birkhäuser, Boston, 1998.

[12] A. Melikyan, P.Bernhard. Geometry of Optimal Paths Around Focal Singular Surfaces in Differential Games. AMO, 2005, vol. 52, pp.23-37.

Department of Mathematics, Virginia Tech, Blacksburg, Virginia 24061
E-mail address: day@math.vt.edu

Institute for Problems in Mechanics, Veradsky Ave. 101-1, 119526 Moscow, Russia
E-mail address: melik@ipmnet.ru